Journal of Chromatography, 630 (1993) 313-327
Elsevier Science Publishers B.V., Amsterdam

CHROM. 24 694

pH gradient simulator for electrophoretic techniques in a Windows environment

Emilio Giaffreda, Carlo Tonani and Pier Giorgio Righetti

Chair of Biochemistry and Department of Biomedical Sciences and Technologies, University of Milan, Via Celoria 2, Milan 20133 (Italy)

(First received July 14th, 1992; revised manuscript received October 19th, 1992)

ABSTRACT

A new program is presented for optimizing mixtures of buffers and titrants for creating pH gradients for isoelectric focusing in immobilized pH gradients and in general for chromatographic processes. The program is written on a windows platform and it includes several novel features compared with previous simulators. First, the estimation of a pH gradient (a non-linear problem) has been transformed into a linear programming problem, thus allowing the use of the simplex as an optimization algorithm. Second, several types of pH gradients can be simulated and optimized, including linear, exponential, logarithmic and sigmoidal. Finally, an equation has been implemented in the program that accounts for the variation of the activity coefficients of ions as a function of the prevailing ionic strength in solution. This simulator was checked experimentally by eluting solutions from a two-vessel gradient mixer and verifying the shape of the various pH gradients. An excellent correlation was found between simulated and experimental data. The program allows the calculation and optimization of pH profiles (including the accompanying ionic strength and buffering power values) for mixtures of up to 50 different monoprotic or oligoprotic buffers and titrants. Calculations and optimizations are performed in a fraction of the time required by previous programs (often in less than 1 min, even for highly complex mixtures).

INTRODUCTION

In contrast to the approximate science represented by isoelectric focusing (IEF) in soluble amphoteric buffers (carrier ampholytes, CAs) (nothing is known on the several hundred chemicals composing wide-pH mixtures and the shape and range of the generated pH gradient is never reproducible) [1], the science dealing with immobilized pH gradients (IPGs) appears to be more precise: the chemicals are well defined and the pH gradient can be engineered as required [2]. This science has been exacting, however: the chemistry of the Immobiline chemicals (acrylamido buffers and titrants grafted to the polyacrylamide matrix) has taken years to develop (see ref. 3 for an update on these compounds) and the calculation of wide-pH recipes has required the development of complex computer algorithms (see ref. 4 for a general survey).

The aim of this paper is to present a new, powerful IPG simulation program, based on the experience we have accumulated in the last 10 years in this field. We shall briefly summarize here what has been developed so far and give the reasons for this latest evolution. Our first simulation program (MGS, or monoprotic electrolyte gradient simulation) was operating by the end of 1982. A first approach to the formation of extended pH gradients was through the sequential elution of buffering species of increasing pK from a five-chamber mixer [5]. This procedure was soon abandoned in favour of standard two-vessel gradient mixing [6,7], for which we studied the conditions for gradient linearity, as a function of the pK distribution of the buffers and of the titrants [7]. We thus produced formulations for a series of wide immobilized pH gradients (spanning 2-6 pH units

Correspondence to: P. G. Righetti, Chair of Biochemistry and Department of Biomedical Sciences and Technologies, University of Milan, Via Celoria 2, Milan 20133, Italy.

0021-9673/93/$06.00

within the pH range 4–10), optimized in terms of gradient linearity [8,9]. We compared [8] two approaches to the generation of extended pH gradients: in one case each buffering Immobiline had the same concentration in both vessels of the mixer; in the other, different concentrations of buffering ions could be present in each chamber.

In the case of two-dimensional (2D) maps, however, the best resolution in the focusing dimension would be obtained by non-linear pH gradients, following the relative abundance of isoelectric proteins along the pH scale. Hence we also calculated wide, non-linear IPG recipes for use in 2D maps and in cases requiring the analysis of highly heterogeneous samples [10].

During 1986, we started to expand the fractionation capability of IPGs: up to that time, the most extended pH interval described was 4–10. For this reason, we had not included the dissociation products of water (H^+ and OH-) in our simulations, because in the pH 4-10 range their concentration is negligible. At that time, we started focusing dansylated amino acids (which exhibited pI values in the pH range 3-4) and we realized that there was a strong divergence between calculated and experimental pH gradients; therefore, our computer program was expanded to include the effects of H^+ and OH^- on the buffering power (β), ionic strength and pH profile [11]. In fact, simulations were not only limited to acidic but also included basic (pH 10-I 1) intervals [12]. As chemicals with more acidic and more basic pK values became available, extended formulations including pH extremes were recently computed; the widest pH range that could be formulated was a 2.5-l 1 interval [13].

During 1988, we started a long-range program on the characterization of existing Immobilines and on the synthesis of new species [3]. The family of Immobilines was thus considerably expanded and our former program (which was limited to mixtures of not more than ten species, including buffers and titrants) could no longer handle the new generation. These factors forced us to develop a new program, PGS (polyelectrolyte gradient simulation), for IEF in IPGs and for chromatography [14,15].

All these programs, however, had some shortcomings, as outlined below.

(a) The approach of minimizing the coefficient of variation of the buffering power [CV(β)], for producing linear pH gradients, is a successful strategy only if the concentration of the Immobiline mixture is constant, *i.e.*, only when the two vessels of the gradient mixer contain the same solution titrated at the two extremes of the pH interval (equal concentration method) [8]; however, more flexibility in recipe calculation is obtained by the "unequal concentration" method, i.e., by using different molarities of the same Immobilines in each vessel. With this latter approach, Righetti *et al.* [16] proposed minimizing SD(pH) (the standard deviation along the pH course) by using the steepest descent principle in the search for buffer concentrations allowing for a better linearity of the pH course.

(b) Minimization of CV(β), although working satisfactorily in the pH range 4–10, cannot perform properly outside these boundaries, where there is a strong contribution of water to the buffering power; as the latter is represented by two branches of a hyperbola, CV(β) as a target function becomes almost meaningless,

(c) Both our previous programs (MGS and PGS, for mono- and polyelectrolytes, respectively) were meant for modelling only linear pH gradients, whereas there are many applications also for non-linear recipes.

Given the above limitations, we have recently expanded our previous programs so as to be able to calculate and optimize not only linear, but also logarithmic, exponential and sigmoidal gradients [17,18]. Another novelty of our latest development was that we abandoned the minimization of CV(β) and adopted as a target function the minimization of the sum of squares of residuals (μ_2). The new simulator performed up to ten times better than our previous programs and could formulate recipes having deviations from linearity well below 1% of the given pH interval (a limit set with the previous MGS and PGS programs).

In this work, we delineate what could possibly be the ultimate step in "pH gradient engineering". The following major improvements have been made: (a) the new program is written under a Windows environment, a most powerful and "user-friendly" program manager; (b) we have been able to adopt, in the optimization algorithm, the simplex method for linear programming (LP), which is much faster and accurate than Monte Carlo or steepest descent procedures; and (c) for the first time, a new algo-

rithm has been introduced that corrects the activity coefficients of ions according to the prevailing ionic strength in solution.

With the latter improvements, we feel that "pH gradient engineering" has now become a numerical science. The program is available from Hoefer Scientific Instruments (654 Minnesota Street, San Francisco, CA 94107, USA).

EXPERIMENTAL

The chemicals listed in Table I were purchased from Fluka (Buchs, Switzerland) and were of analytical-reagent grade.

pH gradient measurements

In order to check the quality of the simulated gradients and for the correction of activity coefficients introduced, we eluted from a two-vessel gradient mixer some simulated mixtures and measured the pH of the fractions. The following procedure was adopted: 60 ml of each limiting solution (corresponding to the "acidic" and "basic" extremes of the pH gradient, respectively) were prepared, degassed, equilibrated under argon and loaded in a two-vessel gradient mixer (the acid solution usually being in the mixing chamber). If the pH gradient extended above pH 7, the alkaline part of the gradient (usually placed in the reservoir) was protected from CO_2 adsorption by flushing with argon. Production of the correct pH gradient on elution was ensured by (a) using a stirrer in both chambers, (b) avoiding glycerol or other additives in the mixing chamber and (c) flushing with argon all eluted fractions above pH 7. Volumes of 2 ml were collected, for a total of 60 fractions. Prior to pH measurements, all fractions were equilibrated at 25°C.

As a gradient mixer, we used that designed by Svensson and Pettersson [19] for isoelectric focusing; stirring action was provided by placing the two electrically driven helices in both vessels simultaneously. The absence of back-flow was checked by visual inspection at the interface of the two solutions, one of them being strongly coloured with bromophenol blue. Linearity of the elution profile was also checked by readings at 600 nm of the blue fraction. Note that, in the absence of a density-forming agent in the mixing chamber (as is customary in gradient mixing), the two solutions are truly hydrostatically equilibrated.

THEORY

The problem of finding a solution to the creation of a linear (or non-linear) pH gradient on mixing two limiting solutions containing a mixture of buffering (and titrant) ions is not trivial. We have already given in previous papers [4–7] all the relevant equations needed for solving the problem ***(i.e.,*** the dissociation of weak acids and bases; the electroneutrality conditions; the total buffering power of the solution; the total ionic strength of the system; and the Peterson-Sober equation allowing the calculation of the actual concentrations dispensed in each liquid element eluted from the mixer). However, a difficult task is the choice of the target function to be extremized and the selection of the proper optimization algorithm working on such a target. In the past, we had chosen, as a target function, the minimization of the coefficient of variation of the buffering capacity [CV(β)], defined as the ratio between the standard deviation of the buffering capacity and its mean value: CV(β) = SD(β)/β. As an alternative method, we had also used, as a goal for maintenance of pH gradient linearity, the minimization of SD(pH). As optimization algorithms, we had already discarded stochastic (also known as Monte Carlo) methods, which utilize random extraction of the vector to be optimized and compute the target function. Unfortunately, stochastic methods usually converge too slowly, rendering their use on personal computers impractical.

We had then opted for the "steepest descent (Cauchy)" algorithm. In this method, the minimum of a function f(k) is found by descending from a given starting point, defined by the parameter vector k^*, along the steepest slope, defined by the minimum value of f'(k*), found by exploring in all directions the space around k^*. After one descending step, the new steepest direction is searched and the process is then iterated until the attainment of the desired minima [20–22]. The most serious drawback of the steepest descent approach is that the search comes to an end when a minimum is reached, regardless of it being an absolute or relative minimum. In order to avoid this, we had provided in previous programs

the possibility of interrupting the routine calculations and allowing educated guesses to be entered by a machine-user interaction procedure. This method also was extremely slow and often computation of complex mixtures encompassing wide pH intervals required several days of calculations.

Ideally, one might want to use the simplex method, by reformulating the objective function, so that it is linear. Linear objective functions then lead automatically to linear programming (LP). In the following section, we shall show how it is possible to transform the problem of pH gradient optimization from a non-linear to a linear case, thus allowing the adoption of the simplex as an optimization algorithm.

Linearization of the problem and the simplex algorithm

We can express the problem as follows: given *m* polyprotic species, of known pK values, and a pH curve, represented by the function pH(t), it is necessary to find an algorithm able to calculate the initial concentrations of the *m* species: $c_{z\mathrm{A}}, c_{z\mathrm{B}}, z = 1,\ldots, m$, to be placed in each chamber of a two-vessel gradient mixer so that, upon linear mixing, the eluate will contain a variable pH (with time), approximating the desired function pH(t). For a solution, the problem will be analysed first from a hydrodynamic point of view, then from its chemical side and finally from a numerical point of view.

Hydrodynamically, if equal volumes of two solutions, one in a mixing chamber (called "acidic", as it contains the lowest pH value) and the other in a reservoir ("basic" solution) are linearly mixed, it can be demonstrated that, for each species $c_{\mathrm{A}}(t)$ in the mixing chamber, the variation in concentration during elution can be expressed by the following differential equation:

$$S\left[\frac{\mathrm{d}}{\mathrm{d}t}\cdot c_{\mathrm{A}}(t)\right]\left[l(0)-\frac{q}{2S}\cdot t\right]=\frac{q}{2}[-c_{\mathrm{A}}(t)+c_{\mathrm{B}}] \qquad (1)$$

where $l(t)$ is the height of the solution in the two chambers, S is the section of each chamber, q is the liquid flux per time unit and c_{B} is the concentration of each species in the basic chamber. On integration, and remembering that the eluted volume V is given by $V =$ (SE), one obtains the explicit form of $c_{\mathrm{A}}(t)$:

$$c_{\mathrm{A}}(t)=c_{\mathrm{A}}\left(1-\frac{q}{2V}\cdot t\right)+\frac{q}{2V}\cdot tc_{\mathrm{B}} \qquad (2)$$

Note that eqn. 2 is the equation of Peterson and Sober [23], simplified for a two-chamber gradient mixer. The same reasoning can be extended to the case of *m* non-interacting species, resulting in the following equation:

$$\sum_{i=1}^{m} c_{i\mathrm{A}}(t)=\sum_{i=1}^{m} c_{i\mathrm{A}}-\frac{q}{2V}\cdot t\sum_{i=1}^{m} c_{i\mathrm{A}}+\frac{q}{2V}\cdot t\sum_{i=1}^{m} c_{i\mathrm{B}} \qquad (3)$$

We have so far treated the hydrodynamic facet of the problem; we shall now proceed to the chemical aspects. We recall here the general equations for the dissociation degrees of polyprotic acids ($\tilde{g}_{\mathrm{a}}$), bases ($\tilde{g}_{\mathrm{b}}$) and zwitterions ($\tilde{g}_{\mathrm{z}}$):

$$\tilde{g}_{\mathrm{a}}(t)=\sum_{i=0}^{n}\alpha_{\mathrm{a}i}(t)(n-i) \qquad (4)$$

$$\tilde{g}_{\mathrm{b}}(t)=\sum_{i=0}^{n}\alpha_{\mathrm{b}i}(t)(n-i) \qquad (5)$$

$$\tilde{g}_{\mathrm{z}}(t)=\tilde{g}_{\mathrm{a}}(t)-\tilde{g}_{\mathrm{b}}(t) \qquad (6)$$

where α_i is the dissociation degree of the ith species and n is the number of protolytic groups. The degree of dissociation, in turn, depends on the pK of each ionizable group, on the prevailing pH in solution and (in our particular solution) on time t. As we know the starting pH in the "acidic" chamber, we shall be able to calculate at each time t the electrolytic equilibrium in this chamber as elution progresses, *i.e., we* can calculate the degree of dissociation of each species as the content of the "acidic" chamber is progressively titrated by the content of the "basic" chamber. By assuming that of the *m* input species I are acids, *p* bases and the remaining zwitterionic, according to the electroneutrality law, it will be

$$-\sum_{i=1}^{l} c_{i\mathrm{A}}(t)\tilde{g}_{i\mathrm{a}}(t)+\sum_{i=l+1}^{l+p} c_{i\mathrm{A}}(t)\tilde{g}_{i\mathrm{b}}(t)+\sum_{i=l+p+1}^{m} c_{i\mathrm{A}}(t)\tilde{g}_{i\mathrm{z}}(t)-[\mathrm{H}^+](t)+\frac{K_{\mathrm{w}}}{[\mathrm{H}^+](t)}=0 \qquad (7)$$

The first member of eqn. 7 can be written as an implicit function, depending on time t and on $2m$ parameters, of the type

$$\mathrm{f}(c_{1\mathrm{A}}, c_{2\mathrm{A}}, \ldots. c_{m\mathrm{A}}, c_{1\mathrm{B}}, c_{2\mathrm{B}}, \ldots. c_{m\mathrm{B}}, t) \qquad (8)$$

which is linear in the parameters $c_{i\mathrm{A}}, c_{i\mathrm{B}}$. The original problem can thus be reduced to the search for the $2m$ parameters $c = (c_{1\mathrm{A}}, c_{2\mathrm{A}}, .., c_{m\mathrm{A}}, c_{1\mathrm{B}}, c_{2\mathrm{B}}, \ldots, c_{m\mathrm{B}})$, such that

$$f(\mathbf{c}, t)\approx 0 \forall t\in[t_0, t_n] \qquad (9)$$

The problem now consists in selecting from a family of functions of the type $f(\boldsymbol{c},t)$ a particular function $f(c^*,t)$ satisfying the condition that, in the interval $[t_1,t_n]$, it will approximate zero. The search for such a function can take two pathways: either exact calculus, or methods of discrete calculus. As the latter seems more manageable, the family of functions $f(\boldsymbol{c},t)$ is now considered as an assembly of discrete functions, defined over the points $\{t_1,\ldots,t_n\}$ rather than over the continuous interval $[t_1,t_n]$. In addition, as f is linear in its $2m$ parameters, the function $f(\boldsymbol{c},t)$ can be rewritten in a vectorial form of the type

$$A \cdot \boldsymbol{c} - \boldsymbol{b} \tag{10}$$

where A is an $n \times 2m$ matrix, c is a $2m$-dimensional vector and b is a n-dimensional vector. Under this terminology, eqn. 9 can be rewritten as follows:

$$\min_{\boldsymbol{c}} ||A \cdot \boldsymbol{c} - \boldsymbol{b}||_p \tag{11}$$

where $||\boldsymbol{e}||_p$ indicates the Lp norm of the vector e [24]. When using the $L1$ norm, the problem can be transformed into a problem of linear programming. In fact, for L_1 approximations, the problem can be reduced to

$$\min \sum_{i=1}^{n} |\boldsymbol{b_i} \sum_{i=1}^{2m} a_{ij}c_j| \tag{12}$$

subject to no restrictions whatsoever. Even though eqn. 12 still does not represent a linear programming problem, it can be easily converted into one. Consider the problem

$$\min \sum_{i=1}^{n} e_i$$

subject to

$$\begin{aligned} e_i + \sum_{j=1}^{2m} a_{ij}c_j &\geqslant b_i \qquad i = 1, 2, \ldots) \text{ n} \\ e_i - \sum_{j=1}^{2m} a_{ij}c_j &\geqslant -b_i \qquad i = 1, 2, \ldots . n \end{aligned} \tag{13}$$

It is not difficult to see that, in an optimum solution $e_1, e_2, \ldots, e_n, c_1, c_2, \ldots, c_{2m}$ of eqn. 13, e_i should be the smallest possible value in between the two bounds $b_i - a_{ij}c_j$ and $b_i + a_{ij}c_j$. Hence,

$$e_i^* = |\boldsymbol{b_i} - \sum_{j=1}^{2m} a_{ij}c_j^*| \tag{14}$$

and the objective function e_i takes the value

$$e_i = \sum_{i=1}^{n} |\boldsymbol{b_i} - \sum_{j=1}^{2m} a_{ij}c_j^*| \tag{15}$$

as desired. We conclude that $c_1, c_2, \ldots, c_n$ is the best L_1 approximation to a solution of eqn. 11. This solution is not the final one, however, as we need the following additional constraints to the program: (a) the sum of concentrations of the m species in the two chambers must be lower than a molarity predetermined by the user; (b) the average β power can also be predetermined by the user (in a linear form, as for the electroneutrality law); and (c) each concentration c_i must be greater than zero. The first condition can be met by adding to eqn. 13 the following constraint:

$$\sum_{i=1}^{m} c_{i\mathrm{A}} \leqslant k \qquad \sum_{i=1}^{m} c_{i\mathrm{B}} \leqslant k \tag{16}$$

The second condition can also be satisfied by adding a constraint to eqn. 13 of the type

$$\sum_{i=1}^{n} \beta(t_i) = n\beta_{\mathrm{M}} \tag{17}$$

where $\beta(t_i)$ is the buffering power of the solution in the acidic chamber at time t and β_{M} is the average β preselected by the user (note that summation of β is used in order to obtain a β average). The last condition is easily met by adding to eqn. 13 the constraint $\boldsymbol{c} \geqslant 0$. At this point, it is clear that the simplex algorithm can be applied to the above problem, as it has now been converted into a linear programming problem.

The simplex, first proposed by Dantzig in 1948 (see ref. 25 for a review), is a powerful optimization algorithm consisting of (a) making a series of linear combinations at each step, so that the value of the target function diminishes, and (b) finding an optimum solution, after a number of iteration steps, which is always smaller than the larger of the two dimensions of the constraint matrix.

The calculus routine finally adopted is that implemented by Kuenzi *et al.* [26].

The problem of the activity coefficients of ions

This is a formidable problem, whch has been avoided in all our previous computations [4–8]. Previously, we assumed that, provided that IPG gels were made to contain small total amounts of

buffering and titrant ions (not exceeding 10 mM), this problem could be neglected. However, in several recipes encompassing wide pH intervals (e.g., 4-8 pH units), and also in Immobiline membranes [27], the total ion molarity grafted in the gel often exceeds 30 mM, which calls for a correction to the activity coefficients of the ions, if an exact science is sought.

The original Debye-Hiickel theory is still the basis for most calculations of activity coefficients. This theory assumes that ions in solution behave as point charges, distributed in a homogeneous dielectric (the solvent); by applying the electrostatic and thermodynamic laws, the Debye-Hiickel relationship is derived, valid only for highly diluted solutions and for fully dissociated ions:

$$-\log\ \gamma = Az_+z_-\sqrt{I} \qquad (18)$$

where γ is the average activity coefficient of a binary electrolyte, z_+ and z_- the respective charges, I the ionic strength and A a constant that depends on the absolute temperature and the dielectric constant of the solvent (for water at 25°C A = 0.509; in many textbooks, A is simply given as 0.5). The experimental results agree with the Debye-Hiickel theory only for concentrations lower than 1 mM. Thus, a modified Debye-Hiickel expression has been derived for higher molarities:

$$-\log\ \gamma = Az^2 \cdot \frac{\sqrt{I}}{1+Ba\sqrt{I}} \qquad (19)$$

where a is a parameter, measured in angstroms, which is roughly proportional to the diameter of a hydrated ion and B is a constant which again depends on the absolute temperature and the dielectric constant of the solvent (for water at 25°C B = 0.328). It should be noted that, if a is taken as 6 Å (which corresponds to the average diameter of a number of ions) the error in the estimation of γ is less than 1% in solutions having I values lower than 0.2 equiv. l^{-1}. In contrast, eqn. 18 does not represent experimental data properly: in solutions up to 0.1 equiv. l^{-1} the error is > 10% (Fig. 1).

Over the years, a number of equations have been derived in an attempt to obtain better γ estimates (see ref. 28 for a review and for additional references to eqns. 20-22). Thus, Guggenheim proposed the following parametric equation:

$$-\log\ \gamma = Az^2 \cdot \frac{\sqrt{I}}{1+\sqrt{I}} - bI \qquad (20)$$

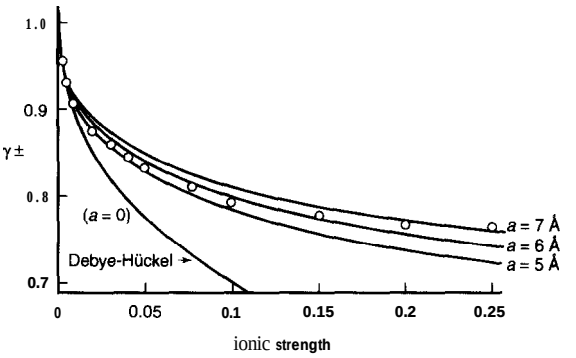

Fig. 1. Theoretical plot of the dependence of activity coefficients on prevailing ionic strength in solution for different ion diameters. Note that, according to the original Debye-Hiickel theory, the diameter of an ion should be zero. In most calculations, however, an average diameter of 6 Å is adopted.

where the average ion diameter has been taken as a = 3 Å (note that, in this case, Ba = 1). A similar equation was proposed by Guntelberg:

$$-\log\ \gamma = Az_+z_-\frac{\sqrt{I}}{1+\sqrt{I}} \qquad (21)$$

based on the same assumption of Ba = 1. Finally, an empirical relationship was derived by Davies:

$$-\log\gamma = Az_+z_-\left(\frac{\sqrt{I}}{1+\sqrt{I}} - 0.21\right) \qquad (22)$$

The dependence of the activity coefficient on the ionic strength, according to eqns. 18, 21 and 22, has been plotted in Fig. 2. It appears that the Davies equation (eqn. 22) follows the experimental data more closely: in solutions of ionic strength up to 0.1 the error is only 3%, and at I up to 0.5 the error is still < 8%.

The situation is even more complex for oligoprotic ions, as shown in Fig. 3. It is seen that, whereas for a monoprotic ion the γ value tends asymptotically to 0.7, at high ionic strength for a divalent ion it decreases dramatically to a limit value of 0.3. For higher valency ions, the fall-off is even more pronounced: for a triprotic ion the asymptotic value is barely 0.05 and for a tetravalent ion the activity coefficient falls off rapidly to zero already at an ionic strength of 0.2.

As will be shown in the Results section, the Davies equation (eqn. 22) seems to lit our experimental data

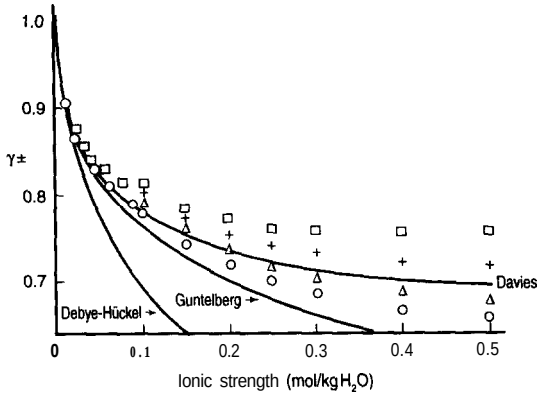

Fig. 2. Plot of the dependence of activity coefficients on prevailing ionic strength in solution according to different equations: Debye–Hückel (eqn. 18), Guntelberg (eqn. 21) and Davies (eqn. 22). Note that the Davies equation is empirical and is based on experimental data for (□) HCI, (+) HNO_3, (A) $NaClO_4$ and (0) KCl.

most satisfactorily, so this equation was incorporated in our computer program for automatic correction of the activity coefficients as a function of the prevailing ionic strength in solution, Since, in practice, when introducing into our computing routines the correction for the activity coefficients, only the stoichiometric constants are altered and the mathematical formulations of equilibria and the mass and charge balance equations are left unaltered, the following two-step computation procedure was adopted. Once a mixture of acids and bases is given, the problem is solved to a first approximation by using the concentrations instead of the activities. Once the final ionic strength of the solution has been derived, the activity coefficients of the various ions are calculated at the given Z value. At this point, new values of p*K* and pH gradients are derived, corrected according to the activity coefficients.

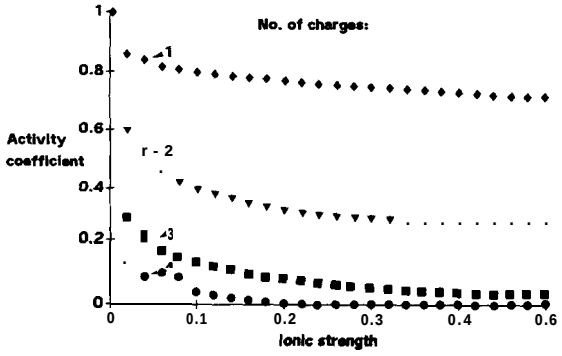

Fig. 3. Plot of the dependence of activity coefficients on prevailing ionic strength in solution for ions of different valency. Note the huge decrease in the coefficients in the transition from monoprotic to diprotic species. Note also how, for a tetravalent ion, the activity coefficient is essentially zero at an ionic strength of 0.2 equiv. l^{-1}.

Program architecture

The above algorithms were implemented in C language under the programming platform Windows 3.0. Windows is a most powerful operating program, which offers the following main innovations: (a) object-oriented programming, (b) message-driven architecture and (c) multitasking. The main "window" usually contains a "title bar", a "menu", a "sizing border", a "system menu icon" and "maximize/minimize icons". The inner area of the main window (or workspace) can be used to generate new "child windows", each containing a document. In our case, we prepared three types of document windows: (a) a first type for handling the input data, ***i.e.,*** the different buffers and titrants with their physico-chemical characteristics (e.g., p*K* values, type of substance, such as acid, base, zwitterion); (b) a second type for handling the input data, and precisely for calculating the molarities of each species to be placed in the "acidic" and "basic" chambers, respectively; this sheet is similar to the previous one, but in addition it will create archives for storage of the optimized recipes for the various pH intervals calculated; and (c) a third type used for the graphic display of simulated recipes and pH intervals.

Examples of the data obtained and experimental validation of the simulations are given below.

RESULTS

Program and simulations

Fig. 4 shows the main dialogue box in our computer program for creating a new mixture and inserting data. It is seen that, in contrast to our previous programs (except for refs. 18 and 19), the user has an option of up to four types of gradients: linear, logarithmic, exponential and sigmoidal. Once

Fig. 4. Dialogue box for data insertion for creation of a new mixture. Note that options are given for the creation of four different types of pH gradients. The other required input data are the starting (lower) and ending (upper) pH values (i.e., the bounds of the pH interval to be generated), the maximum total molarity of all species in solution and the average desired β power along the eluted pH gradient.

the type of gradients is selected, the program needs, as input data, the lower starting pH (i.e., the desired pH of the solution that will be placed in the "acidic" or mixing chamber) and the upper pH (i.e., the pH of the solution which will fill the "basic" chamber, or reservoir). Important options given to the user are (a) the selection of maximum-total molarity (as a sum of the partial molarity of each ion in solution) and (b) the selection of the mean β power along the pH gradient.

TABLE I

LIST OF BUFFERS (WITH RESPECTIVE pK VALUES) USED IN MODELLING AND MEASURING pH GRADIENTS

No.	Name	Type	pK values
1	HCl[a]	Acid	0.4
2	Citric acid	Acid	3.128, 4.762, 6.4
3	Chloroacetic acid	Acid	2.92
4	Itaconic acid	Acid	3.85, 5.45
5	Acetic acid	Acid	4.75
6	Malonic acid	Acid	2.83, 5.69
7	Sulphanilic acid	Acid	3.23
8	Glutaric acid	Acid	4.31. 5.41
9	Tris base	Base	8.3
10	Imidazole	Base	6.9
11	NaOH[a]	Base	13
12	Diethylamine	Base	10.489
13	Piperazine	Base	9.83
14	Quinine	Base	8.52
15	Azetidine	Base	11.29
16	Pilocarpine	Base	6.87

[a] For computational purposes HCl was assigned pK = 0.4 and NaOH pK = 13.

TABLE II

OPTIMIZED RECIPE FOR CREATION OF A LINEAR pH 3-11 GRADIENT, AS PLOTTED IN FIG. 5

No.	Name	Chamber A (mM)	Chamber B (mM)
1	HCl	30.134	0.000
2	Citric acid	2.822	9.685
3	Chloroacetic acid	0.000	0.000
4	Itaconic acid	4.253	0.000
5	Acetic acid	0.000	0.000
6	Malonic acid	0.000	0.000
7	Sulphanilic acid	1.021	5.143
8	Glutaric acid	0.000	0.000
9	Tris base	4.324	4.051
10	Imidazole	0.000	8.086
11	NaOH	0.000	33.308
12	Diethylamine	0.000	6.164
13	Piperazine	23.833	1.913
14	Quinine	0.000	1.650
15	Azetidine	0.000	0.000
16	Pilocarpine	3.613	0.000

We shall now give some examples of different types of gradients that can be generated by our computer program. Table I gives a mixture of sixteen common acids and bases (weak and strong), some oligoprotic and most monoprotic (pK values as given in refs. 29 and 30). These tables can be prepared and stored by the user as databases. Table11 gives the same kind of table, with already calculated and optimized molarities of all components for creation of a linear pH 3-l 1 gradient with the following preset requirements: maximum total molarity of all ions, 100 mM; and average β, 6 mequiv. l^{-1} pH^{-1}. It should be noted that everything is done automatically by the computing algorithms: thus, during the calculations and optimization, some components are automatically excluded by the mixture, since their pK values would hamper the generation of a linear gradient. In this particular case, components 3, 5, 6, 8 and 15 have been automatically excluded from the mixture. The resulting gradient is shown in Fig. 5; it is seen that,

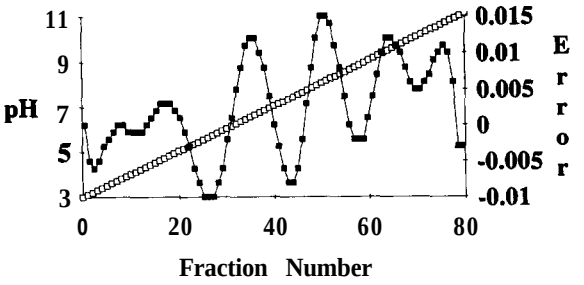

Fig. 5. Simulation of (□) the pH gradient profile and (■) deviation from linearity of the mixture in Table II. Parameters of the gradient: linear pH 3-l 1 gradient; maximum total molarity, 100 mM; average β, 6 mequiv. $l^{-1}pH^{-1}$. Note the minute deviations from linearity and their constant oscillations around zero.

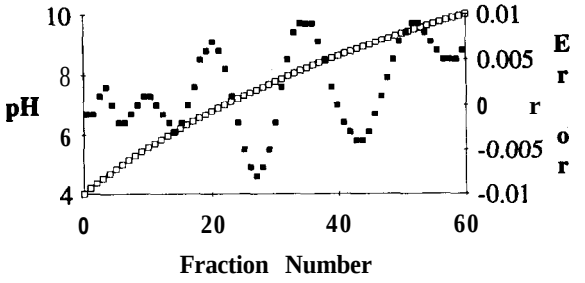

Fig. 6. Simulation of (□) the pH gradient profile and (■) deviation from the desired shape of the mixture in Table III. Parameters of the gradient: logarithmic pH 4–10 gradient; maximum total molarity, 50 mM; average β, 6 mequiv. $l^{-1}pH^{-1}$.

by linear elution, from a two-vessel gradient mixer, of two equal volumes of the compositions as given in Table II for the "acidic" and "basic" chambers, a remarkably linear pH gradient is obtained. The deviations from linearity are extremely minute, and are well below 1% of the width of the generated pH interval, a limit given in previous calculations [4–8].

Table III gives the same mixture, but for the calculation of a logarithmic gradient spanning the pH range 4–10, with the following constraints: maximum total molarity of all ions, 50 mM; and average β power along the pH gradient, 6 mequiv. $l^{-1}pH^{-1}$. The gradient thus formed is shown in Fig. 6; it is seen that the pH profile has the desired shape and that again the deviation (this time from the desired logarithmic shape) is still minute. Note in Fig. 6, as in Fig. 5, how the deviations oscillate constantly around zero in an almost sinusoidal fashion, a prerequisite for minimizing this function [17,18].

TABLE III

OPTIMIZED RECIPE FOR CREATION OF A LOGARITHMIC pH 4-10 GRADIENT, AS PLOTTED IN FIG. 6

No.	Name	Chamber A (mM)	Chamber B (mM)
1	HCl	18.129	0.000
2	Citric acid	4.083	5.794
3	Chloroacetic acid	0.000	0.000
4	Itaconic acid	0.000	0.000
5	Acetic acid	0.000	0.000
6	Malonic acid	2.521	0.000
7	Sulphanilic acid	0.000	0.000
8	Glutaric acid	0.000	0.000
9	Tris base	9.363	0.000
10	Imidazole	0.000	11.203
11	NaOH	0.000	11.380
12	Diethylamine	0.000	0.000
13	Piperazine	10.181	11.816
14	Quinine	0.000	9.852
15	Azetidine	0.000	0.000
16	Pilocarpine	5.718	0.000

TABLE IV

OPTIMIZED RECIPE FOR CREATION OF A CONCAVE EXPONENTIAL pH 4-10 GRADIENT, AS PLOTTED IN FIG. 1

No.	Name	Chamber A (mM)	Chamber B (mM)
1	HCl	14.360	0.000
2	Citric acid	0.000	14.958
3	Chloroacetic acid	0.000	0.000
4	Itaconic acid	0.000	2.780
5	Acetic acid	0.000	0.000
6	Malonic acid	0.000	3.338
7	Sulphanilic acid	30.632	3.797
8	Glutaric acid	9.029	0.000
9	Tris base	9.033	2.764
10	Imidazole	0.000	0.000
11	NaOH	0.000	57.530
12	Diethylamine	0.000	0.000
13	Piperazine	34.829	6.709
14	Quinine	0.000	0.939
15	Azetidine	0.000	0.000
16	Pilocarpine	2.117	7.135

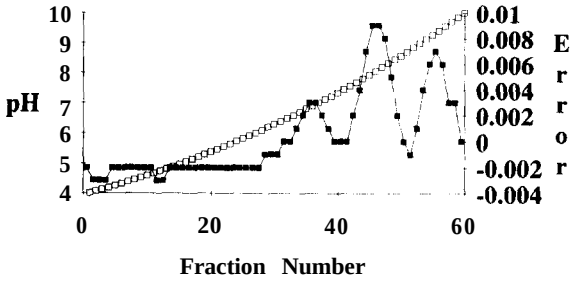

Fig. 7. Simulation of (□) the pH gradient profile and (■) deviation from the desired shape of the mixture in Table IV. Parameters of the gradient: exponential pH 4–10 gradient; maximum total molarity, 100 m*M*; average β, 6 mequiv. l^{-1} pH^{-1}.

Table IV gives again the same mixture, but for the calculation of a concave exponential pH 4–10 gradient with the following constraints: maximum total molarity of all ions, 100 m*M*; and average β power along the pH gradient, 6 mequiv. $l^{-1}pH^{-1}$. The gradient thus formed is shown in Fig. 7; here too the minute deviation from the desired shape should be appreciated. Such deviations (of barely a few thousandths of a pH unit) cannot be appreciated even by the most sensitive pH meters.

Experimental validation of the activity coefficient corrections

We have seen above that it is possible to select different shapes of pH gradients, and that such shapes are automatically calculated and optimized by our simulator in extremely short times (usually in less than 1 min). It remains to be seen whether the activity coefficient corrections we have implemented (the Davies equation) have any practical meaning and can be reproduced in routine work. We therefore explored how the Davies equation applies in different cases, such as conditions of low to very

TABLE V

OPTIMIZED RECIPE FOR A pH 3.3–6.6 GRADIENT (MAXIMUM MOLARITY 75 m*M* PER CHAMBER, MEAN BUFFERING POWER 14 mequiv. $l^{-1}pH^{-1}$)

Recipe used for modelling the pH gradient in Fig. 8

Name	Chamber 1 (m*M*)	Chamber 2 (m*M*)
Chloroacetic acid	3.415	0.000
Itaconic acid	16.35	16.03
Acetic acid	10.28	9.81
Imidazole	4.17	46.69

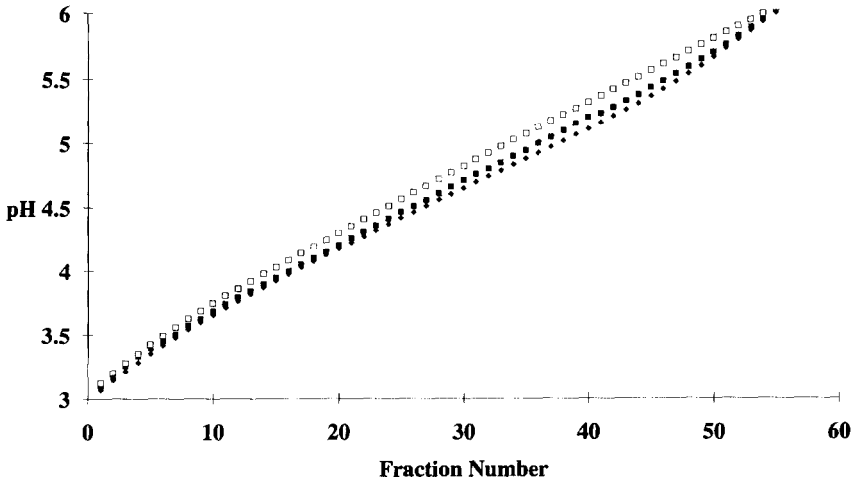

Fig. 8. Comparison between simulated and experimental pH profiles. A pH 3.3–6.3 gradient was generated according to the recipe in Table V. Constraints: maximum molarity (in each chamber), 75 m*M*; average β power, 14 mequiv. l^{-1} pH^{1} Sixty 2-ml fractions were eluted and the pH carefully measured at 25°C in a thermostated vessel (■ = pH-measured). The simulated pH profiles, with (◆ = pH-Davies) and without (□ = pH-NoCorr) Davies correction, are also plotted. Note the divergence between the two simulated profiles and the good agreement between experimental and Davies-corrected simulations.

TABLE VI

EXAMPLE OF THE CALCULATIONS PERFORMED ON ELUTED FRACTIONS FOR THE pH GRADIENT PLOTTED IN FIG. 8

Abbreviations: meas. = fraction number; pH-meas. = experimentally measured pH gradient; pH-NoCorr. = simulated pH gradient without any correction; pH-Huck. = pH gradient simulated with the Debye–Hückel correction; pH-Davies = pH gradient simulated with the Davies correction; I = ionic strength of each fraction (expressed in equiv. l^{-1}); β = buffering power (expressed in mequiv. l^{-1} pH^{-1}).

Meas.	pH-meas.	pH-NoCorr.	pH-Huck.	pH-Davies	*I*	β
1	3.098	3.121	3.068	3.065	0.00556	9.568
2	3.171	3.202	3.143	3.14	0.00611	9.898
3	3.258	3.279	3.216	3.213	0.00668	10.288
4	3.335	3.354	3.287	3.283	0.00726	10.715
5	3.395	3.425	3.354	3.35	0.00786	11.159
6	3.453	3.494	3.419	3.414	0.00847	11.601
1	3.504	3.56	3.481	3.476	0.00909	12.027
8	3.571	3.624	3.541	3.536	0.00973	12.426
9	3.622	3.685	3.6	3.594	0.01039	12.788
10	3.683	3.745	3.656	3.65	0.01105	13.11
11	3.14	3.804	3.712	3.705	0.01173	13.389
12	3.792	3.861	3.766	3.759	0.01242	13.623
13	3.842	3.918	3.819	3.812	0.01312	13.814
14	3.893	3.974	3.871	3.864	0.01384	13.965
15	3.946	4.029	3.923	3.915	0.01457	14.081
16	3.996	4.083	3.974	3.966	0.0153	14.167
17	4.049	4.138	4.025	4.016	0.01605	14.229
18	4.101	4.192	4.075	4.066	0.01681	14.272
19	4.152	4.246	4.125	4.115	0.01759	14.303
20	4.203	4.299	4.174	4.164	0.01837	14.326
21	4.259	4.353	4.224	4.213	0.01917	14.347
22	4.306	4.406	4.272	4.261	0.01999	14.369
23	4.351	4.459	4.321	4.309	0.02082	14.393
24	4.411	4.511	4.369	4.357	0.02166	14.423
25	4.464	4.564	4.417	4.404	0.02252	14.458
26	4.509	4.616	4.464	4.45	0.02341	14.497
21	4.555	4.668	4.511	4.497	0.02431	14.54
28	4.608	4.12	4.558	4.543	0.02523	14.585
29	4.66	4.771	4.604	4.589	0.02617	14.631
30	4.712	4.822	4.65	4.634	0.02713	14.677
31	4.758	4.872	4.696	4.679	0.02811	14.719
32	4.8	4.923	4.742	4.724	0.02911	14.757
33	4.847	4.973	4.787	4.769	0.03014	14.788
34	4.894	5.023	4.832	4.813	0.03118	14.81
35	4.942	5.072	4.878	4.858	0.03224	14.819
36	4.996	5.122	4.923	4.903	0.03332	14.814
37	5.043	5.171	4.969	4.948	0.03441	14.791
38	5.096	5.22	5.015	4.994	0.03551	14.746
39	5.148	5.269	5.062	5.04	0.03661	14.677
40	5.2	5.318	5.11	5.087	0.03772	14.581
41	5.23	5.367	5.158	5.135	0.03883	14.456
42	5.215	5.416	5.207	5.184	0.03993	14.302
43	5.329	5.465	5.258	5.234	0.04102	14.12
44	5.311	5.514	5.31	5.287	0.04208	13.913
45	5.429	5.563	5.364	5.34	0.04313	13.685
46	5.481	5.612	5.42	5.397	0.04415	13.444
47	5.539	5.661	5.478	5.455	0.04513	13.204

(Continued on p. 324)

TABLE VI *(continued)*

Meas.	pH-meas.	pH-NoCorr.	pH-Huck.	pH-Davies	I	β
48	5.591	5.71	5.538	5.516	0.04607	12.976
49	5.648	5.759	5.6	5.58	0.04697	12.78
50	5.699	5.807	5.665	5.647	0.04781	12.635
51	5.759	5.855	5.732	5.716	0.04861	12.56
52	5.826	5.901	5.8	5.787	0.04935	12.576
53	5.89	5.947	5.868	5.858	0.05003	12.696
54	5.964	5.992	5.936	5.93	0.05064	12.93 1
55	6.032	6.035	6.002	5.999	0.05119	13.282
56	6.094	6.077	6.066	6.066	0.05168	13.745
57	6.151	6.117	6.126	6.129	0.05209	14.31
58	6.208	6.156	6.183	6.188	0.05244	14.963
59	6.261	6.193	6.236	6.243	0.05271	15.69
60	6.308	6.228	6.285	6.294	0.05292	16.476

high ionic strength and narrow and wide pH gradients.

Fig. 8 gives the pH profiles generated by computer simulation without (open boxes) and with (diamonds) the Davies correction. The starting mixture spans the pH interval 3.3-6.3 and has the following constraints: maximum molarity (in each chamber), 75 mM; and average β power, 14 mequiv. l^{-1} pH^{-1}. This mixture was selected so as to avoid CO_2 adsorption and as a representative low ionic strength recipe (as given in Table V). In parallel to the simulation, 60 ml of each of the two solutions were prepared, loaded in a two-vessel gradient mixer and eluted, collecting 2 ml per fraction.

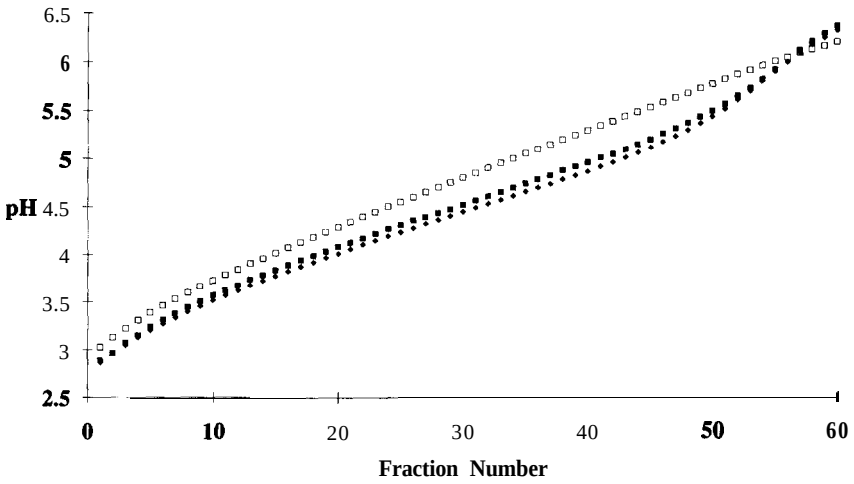

Fig. 9. Comparison between simulated and experimental pH profiles. A pH 3.3–6.3 gradient was generated according to the recipe in Table V (with a tenfold increase in molarity of each ion). Constraints: maximum molarity (in each chamber), 750 mM; average β power, 140 mequiv. l^{-1} pH^{-1}. Sixty 2-ml fractions were eluted and the pH carefully measured at 25°C in a thermostated vessel (■ = pH-measured). The simulated pH profiles, with (◆ = pH-Davies) and without (□ = pH-NoCorr) Davies correction, are also plotted.

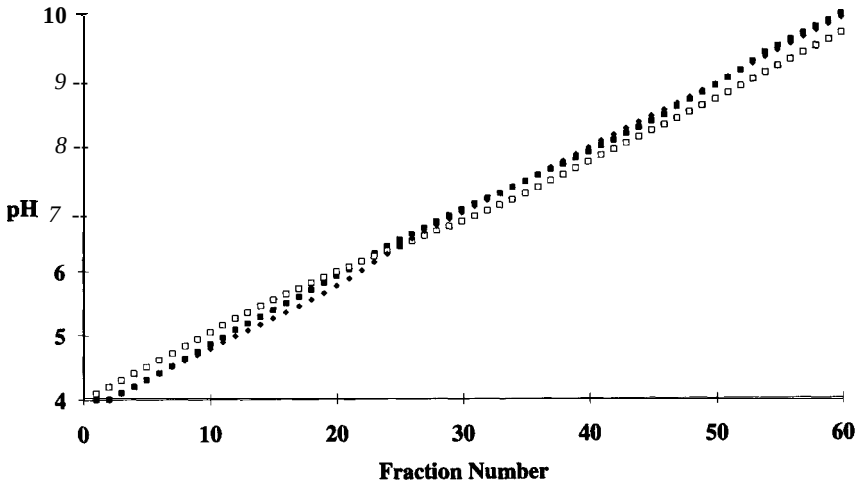

Fig. 10. Comparison between simulated and experimental pH profiles. A pH 4–10 gradient was generated according to the recipe in Table VII. Constraints: maximum molarity (in each chamber), 200 m*M*; average β power, 15 mequiv. $l^{-1}pH^{-1}$. Sixty 2-ml fractions were eluted and the pH carefully measured at 25°C in a thermostated vessel (■ = pH-measured). The simulated pH profiles, with (◆ = pH-Davies) and without (□ = pH-NoCorr) Davies correction, are also plotted.

Two phenomena are immediately apparent: there is a strong divergence between the two computed pH profiles in the absence and presence of the Davies correction, and the real pH gradient, as eluted from the gradient mixer, follows closely the simulated profile with the Davies correction. Note that the divergence between the two simulated profiles follows closely the prevailing ionic strength of the eluted fractions; thus, as the total ionic strength increases (towards the basic end of the gradient, owing to progressive deprotonation of weak acids), the divergence increases from only 0.1 pH unit (between fractions 10 and 20) to as high as 0.2 pH unit (between fractions 40 and 50) (see also the corresponding Table VI, which gives the main parameters of each eluted fraction).

TABLE VII

OPTIMIZED RECIPE FOR A pH 4.0–10.0 GRADIENT (MAXIMUM MOLARITY 200 m*M* PER CHAMBER, MEAN BUFFERING POWER 15 mequiv. $l^{-1}pH^{-1}$)

Recipe used for modelling the pH gradient in Fig. 10.

Name	Chamber 1 (m*M*)	Chamber 2 (m*M*)
Chloroacetic acid	106.8	21.19
Itaconic acid	0.00	57.55
Acetic acid	15.04	0.00
Imidazole	30.06	0.00
Tris base	53.16	9.115
Diethanolamine	19.64	1.975
Ethanolamine	0.00	32.98
NaOH	0.00	126.6

At this point, it is of interest to see what happens to the same mixture at a much increased ionic strength. We therefore took the mixture in Table V and multiplied all the molarity values by a factor of 10. In this new mixture (still encompassing the pH interval 3.3-6.3) the new parameters are therefore maximum total molarity (in each chamber) 750 m*M* and average β power 140 mequiv. $l^{-1}pH^{-1}$. Fig. 9 shows the new simulated pH profiles; now the divergence between the two profiles (with and without correction) is much more pronounced (up to 0.45 pH unit in the region of maximum ionic strength, i.e., fractions 40–50). Here again it can be appreciated that the experimental, measured pH in the eluted fractions follows very closely the Davies-corrected profile.

We next explored whether the corrections adopted apply also in extended pH intervals and in alkaline pH ranges. A new recipe was prepared (see Table VII) encompassing the pH range 4-10, with the following

constraints: maximum molarity (per chamber), 200 mM and average β power, 1.5 mequiv. l^{-1} pH^{1}. As shown in Fig. 10, the simulated patterns follow very closely those obtained previously (Figs. 8 and 9); in the acidic part of the gradient, the two simulated profiles (with and without Davies correction) diverge, the latter being higher than the former; around neutrality, there is a cross-over (as clearly hinted in the upper parts of the graphs depicted in Figs. 8 and 9) and at alkaline pH the Davies-corrected (and experimentally measured) pH courses run higher than the uncorrected ones. We can therefore conclude, from the experimental evidence presented here, that the correction algorithm proposed fulfils the expectations.

DISCUSSION

The simulator presented here has some unique features compared with previous programs [4–7] 'that are worth highlighting. First, we have been able to introduce, as an optimization algorithm, the simplex, one of the most powerful and fastest for this kind of task. We had discarded the simplex in all our previous simulations on the grounds that it cannot be applied to solving non-linear problems. We were therefore forced to adopt mathematical transformations of all the basic equations, so as to transform a non-linear into a linear programming problem. That we are on correct grounds was also checked by resimulating all our optimized mixtures with the other available programs and also by experimentally eluting the simulated gradients and checking the pH values of the collected fractions.

The advantages of the simplex are several. First, it finds the exact solution to the problem. Second, it is much quicker than other optimization methods we had adopted in the past. For example, in our early programs [5,8], based on Cauchy's steepest descent algorithm, the calculations were extremely slow; thus, for calculating and optimizing a pH 4-10 recipe (containing only six or seven species) often >24 h were required, and sometimes the ideal solution could not be found, so that the user had to stop the program and enter educated guesses (for varying the molarity of the different species). Enormous progress was already made with the recent work of Tonani and Righetti [17,18], the direct precursor of the present program, in which the calculation routines were reduced to only 10–15 min.

Another unique feature of our program is the introduction of the Davies equation for correcting the activity coefficient of ions as a function of the prevailing ionic strength in solution. As the preparation of immobilized pH gradients has been claimed to be finally an exact science [2], able to overcome all the defects and imprecisions connected with conventional isoelectric focusing in soluble, amphoteric buffers [1], all sources of errors have to be removed, if "pH gradient engineering" is aimed for. In addition, in IPGs, it is customary to measure the isoelectric point of a protein by a simple interpolation procedure along a pH gradient with a well known profile. A precision of ± 0.01 pH unit is generally claimed.

All the above cannot be completely valid unless extra effort is made to eliminate the last source of uncertainty, *i.e.*, the variation of activity coefficients as a function of ionic strength. It is known that, as the ionic strength in solution is increased, the diffuse double layer around an ion "shrinks" and progressively moves close to the rigid layer. Among the effects of such a phenomenon is a small, but non-negligible, pK change of the weak anions and cations in solution. As the recipes we formulate assume "constant pK values", if the latter assumption is no longer valid one would expect a shift of the generated pH gradient. This shift is in general small (perhaps of the order of a few hundredths of a pH unit) at small values of ionic strength in solution. As in general our IPG recipes were made to contain not more than 10 mM buffering ion, we had in the past neglected such corrections. However, the deviation becomes appreciable at higher buffer and titrant molarities: we have seen (Fig. 8) that even with 75 mM total ions in solution the discrepancy between the simulated and experimental pH curves is as high as 0.2 pH unit. At molarities >700 mM, this discrepancy is as high as 0.45 pH unit. In many recipes proposed today the total ion molarity often exceeds 50 mM, so it seems impossible to continue to ignore such corrections.

We therefore tested the various corrections proposed (see eqns. 18-22) and it seems safe to conclude, from our data, that the Davies correction more closely follows the experimental pH gradient obtained. We therefore feel that the present program

is a major step in rendering "pH gradient" engineering an exact science. Needless to say, although our knowledge has mostly been applied, in this decade, to the generation and optimization of immobilized pH gradients to be used under isoelectric focusing conditions, it is implicit that this know-how is valid in all other instances, e.g., for generating pH gradients in ion-exchange chromatography and in all problems of titration.

ACKNOWLEDGEMENTS

This work was supported in part by grants from the Agenzia Spaziale Italiana (AS), Consiglio Nazionale delle Ricerche (CNR, Rome, Italy), Progetti Finalizzati Biotecnologie e Biostrumentazione, Chimica Fine II e FATMA. We thank Dr. Marco Fazio for help with pH gradient measurements.

REFERENCES

1 P. G. Righetti, ***Isoelectric Focusing: Theory, Methodology and Applications,*** Elsevier, Amsterdam, 1983.
2 P. G. Righetti, ***Immobilized pH Gradients: Theory and Methodology,*** Elsevier, Amsterdam, 1990.
3 M. Chiari and P. G. Righetti, ***Electrophoresis, 13 (1992) 187-191.***
4 F. C. Celentano, E. Gianazza and P. G. Righetti, *Electrophoresis, 12 (1991)* 693–703.
5 ***G.*** Dossi, F. Celentano, E. Gianazza and P. G. Righetti, ***J. Biochem. Riophys. Methods, 7 (1983) 123-142.***
6 E. Gianazza, G. Dossi, F. Celentano and P. G. Righetti, ***J. Biochem. Riophys. Methods, 8 (1983)*** 109–133.
7 F. C. Celentano, E. Gianazza, G. Dossi and P. G. Righetti, ***Chemometr.*** *Intell. Lab. Syst.*, 1 (1987) 349-358.
8 E. Gianazza, F. C. Celentano, G. Dossi, B. Bjellqvist and P. G. Righetti, ***Electrophoresis, 5 (1984) 88-97.***
9 E. Gianazza, S. Astrua-Testori and P. G. Righetti, *Electrophoresis, 6 (1985)* 113-l 17.
10 E. Gianazza, P. Giacon, B. Sahlin and P. G. Righetti, ***Electrophoresis, 6 (1985) 53-56.***
11 P. G. Righetti, E. Gianazza and F. C. Celentano, ***J. Chromatogr., 356 (1986) 9-14.***
12 R. A. Mosher, M. Bier and P. G. Righetti, ***Electrophoresis, 7 (1986) 59-66.***
13 E. Gianazza, F. C. Celentano, S. Magenes, C. Ettori and P. G. Righetti, ***Electrophoresis,*** 10 (1989) 806–808.
14 F. C. Celentano, C. Tonani, M. Fazio, E. Gianazza and P. G. Righetti, ***J. Biochem. Biophys. Methods, 16 (1988)*** 109–128.
15 P. G. Righetti. M. Fazio, C. Tonani, E. Gianazza and F. C. Celentano, ***J. Biochem. Biophys. Methods, 16 (1988) 129-140.***
16 P. G. Righetti, E. Gianazza and C. Gelfi, in V. Neuhoff (Editor), ***Electrophoresis '84,*** VCH, Weinheim, 1984, pp. 29-48.
17 C. Tonani and P. G. Righetti, ***Elecfrophoresis, 12 (1991) 1011-1021.***
18 P. G. Righetti and C. Tonani, ***Electrophoresis, 12 (1991) 1021-1027.***
19 H. Svensson and S. Pettersson, Sep. ***Sci.,*** 3 (1968) 209–215.
20 R. I. Jennrich and M. L. Ralston, ***Annu. Rev. Biophys. Bioeng.,*** 8 (1979) 195-238.
21 W. J. Kennedy and J. E. Gentle, ***Statistical Computing,*** Marcel Dekker, New York, 1980.
22 D. A. Ratkowsky, ***Non-Linear Regression Modelling,*** Marcel Dekker, New York, 1983.
23 E. A. Peterson and H. A. Sober, in P. Alexander and A. Block (Editors), ***Analytical Methods of Protein Chemistry I,*** Pergamon Press, New York, 1960, pp.88–102.
24 P. G. Ciarlet and J. L. Lions, ***Handbook of Numerical Analysis,*** Elsevier, Amsterdam, 1990.
25 D. J. Leggett, ***J. Chem. Educ., 60 (1983)*** 707–710.
26 A. Kuenzi, L. Tzschach and M. Zehnder, in W. H. Press, B. P. Flannery, S. A. Teukolsky and W. T. Vetterling (Editors), ***Numerical Recipes in C. The Art of Scientific Computing,*** Cambridge University Press, Cambridge, 1987, pp. 276 and 290.
27 P. G. Righetti, E. Wenisch and M. Faupel, ***J. Chromatogr., 475 (1989) 293-309.***
28 J. N. Butler, ***Ionic Equilibrium,*** Addison-Wesley, New York, 1964, pp. 457479.
29 R. G. Bates, ***Determination of*** *pH:* ***Theory and Practice,*** Wiley, New York, 1973.
30 R. C. Weast (Editor), ***CRC Handbook of Chemistry and Physics,*** CRC Press, Boca Raton, FL, 67th ed., 1987, pp. D159–D164.